Journal Name

ARTICLE

Supplementary

Design of interfaces in efficient $Ln_2NiO_{4+\delta}$ (Ln = La, Pr) cathode for SOFCs application

R. K. Sharma[a, b, c], M. Burriel[d], L. Dessemond[a, b], J.M. Bassat[c], E. Djurado[a, b*]

[a.] *Univ. Grenoble Alpes, LEPMI, F-38000 Grenoble, France*
[b.] *CNRS, LEPMI, F-38000 Grenoble, France*
[c.] *ICMCB, CNRS, Université Bordeaux, 33608 PESSAC, France*
[d.] *Univ. Grenoble Alpes, CNRS, LMGP, F-38000 Grenoble, France*

* Corresponding author, Phone: +33-476826684; Fax: +33-476826777
E-mail: elisabeth.djurado@lepmi.grenoble-inp.fr

FULLPROF refinement of the XRD patterns of the $Ln_2NiO_{4+\delta}$ (Ln = La, Pr) films prepared by ESD on a screen printed CGO layer on a CGO pellet.

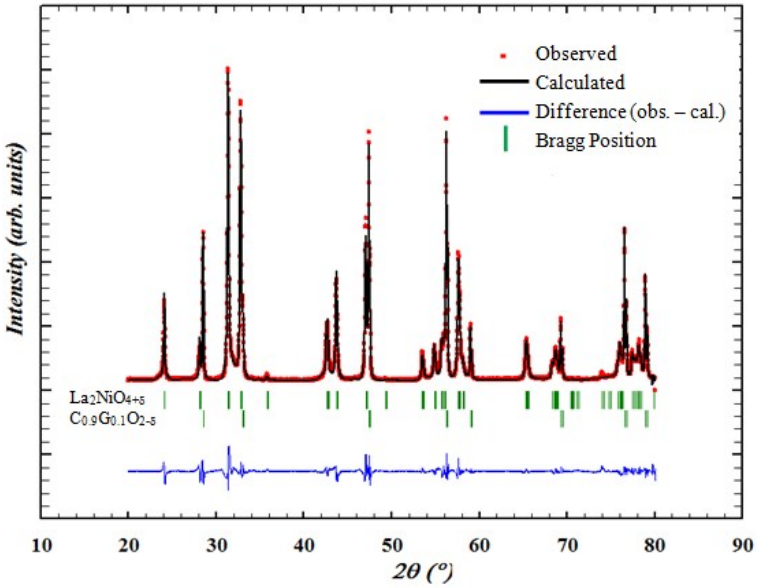

Fig. S1 FULLPROF refinement of the XRD patterns of $La_2NiO_{4+\delta}$ film deposited by ESD on a screen printed CGO layer on a CGO pellet (Fit parameters: χ^2 = 12.2, Bragg R-factor = 1.272 and RF-factor = 0.637 for $La_2NiO_{4+\delta}$; Bragg R-factor = 0.925 and RF-factor = 0.442 for CGO).

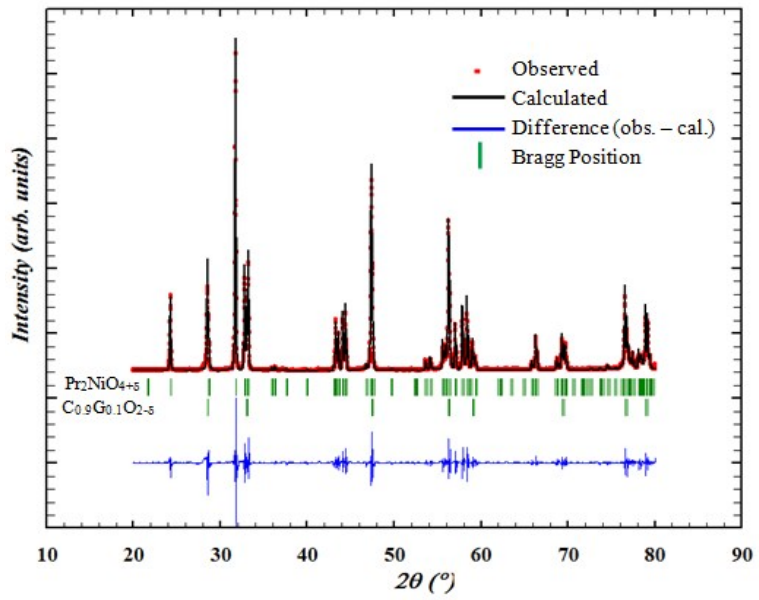

Fig. S2 FULLPROF refinement of the XRD patterns of $Pr_2NiO_{4+\delta}$ film deposited by ESD on a screen printed CGO layer on a CGO pellet (Fit parameters: χ^2 = 26.2, Bragg R-factor = 1.13 and RF-factor = 0.601 for $Pr_2NiO_{4+\delta}$; Bragg R-factor = 0.556 and RF-factor = 0.319 for CGO).

Oxygen overstoichiometry by TGA:

TGA curves of $La_2NiO_{4+\delta}$ and $Pr_2NiO_{4+\delta}$ are shown in **Fig. S3**. Two weight changes are observed: the first one occurs around 350 °C, corresponding to the reduction of Ni^{3+} into Ni^{2+} (the oxygen overstoichiometry being reduced down to $\delta = 0$). The second weight loss characterizes the complete reduction of LnNO into La_2O_3, Pr_2O_3 and Ni. The δ value has been calculated from both values of the weight changes using mole conservation principle.

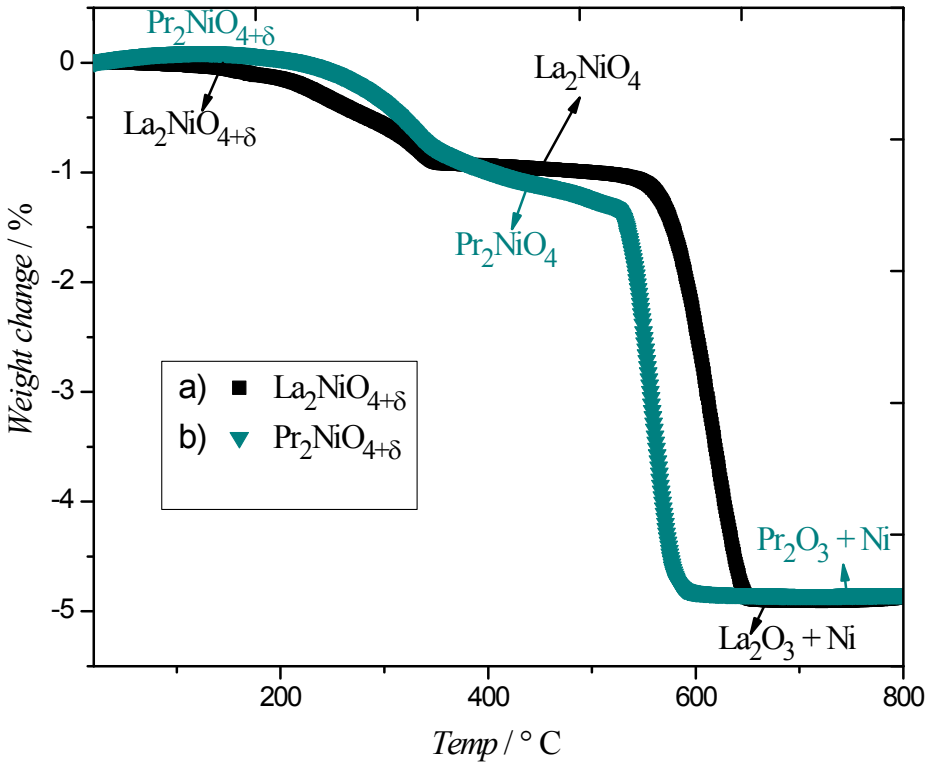

Fig. S3 TGA curves of $La_2NiO_{4+\delta}$ and $Pr_2NiO_{4+\delta}$.

Micrographs of sample 5:

Fig. S4 shows the SEM micrographs of sample 5, the LaNO cross section and the CGO-LaNO composite base-layer of the LaNO triple layer design on CGO substrate using sequentially SP and ESD.

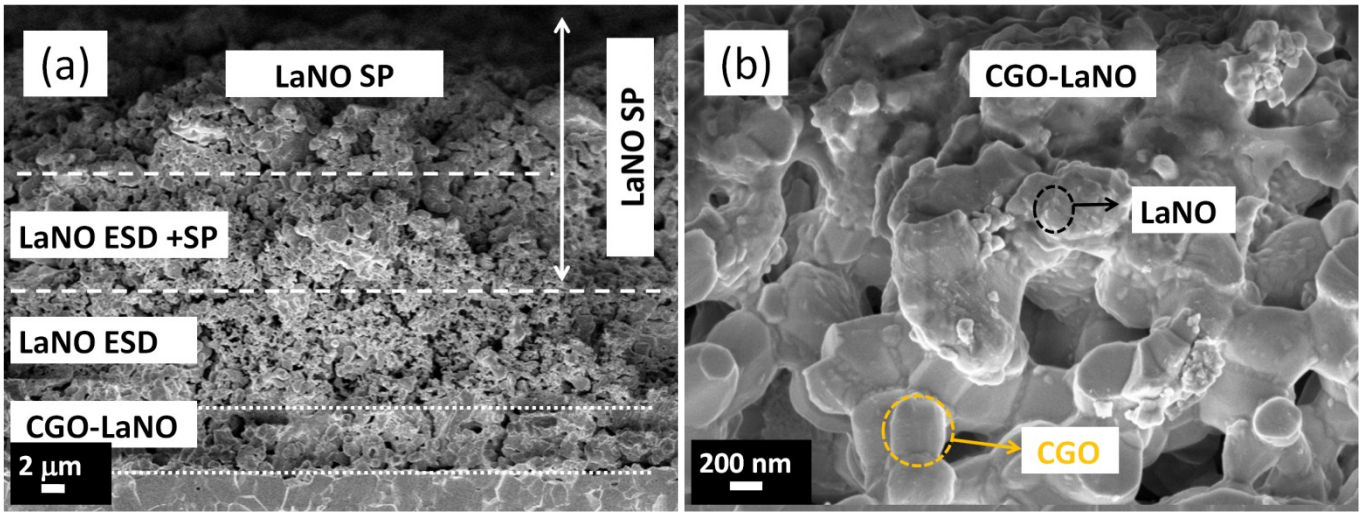

Fig. S4 SEM micrographs of sample 5: (a) cross section, (b) CGO-LaNO sub-layer on CGO electrolyte.

The experimental and fitted impedance spectra at 600 °C from the inset of **Fig. 8b**, is shown in **Fig. S5** along with capacitances and exponents of CPE for all 6 architectures in Table S1.

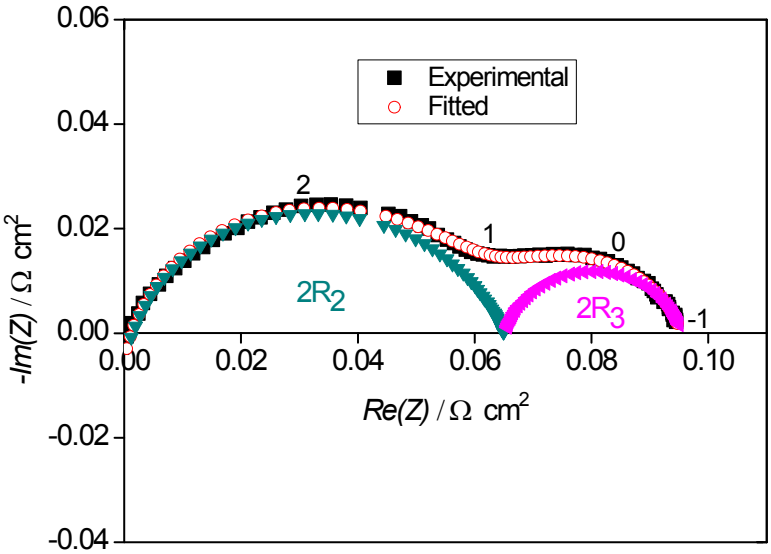

Fig. S5 Nyquist plots recorded at 600 °C in air at OCV for sample 6. The numbers indicate the logarithm of the measuring frequency.

Table S1 Capacitances (F cm^{-2}) and exponents of CPE for all six architectures (estimated error is < 5 %).

Sample	CPE_1			CPE_2			CPE_3		
	n	Q	C_1	n	Q	C_2	n	Q	C_3
Sample 1	0.5552	0.0051	$5.8x10^{-5}$	0.8224	0.0022	$3.3x10^{-3}$	-----	-----	-----
Sample 2	0.8805	0.0049	$9.3x10^{-4}$	0.9036	0.0063	$1.8x10^{-3}$	-----	-----	-----
Sample 3	0.7529	0.0092	$7.1x10^{-4}$	0.8062	0.0074	$1.2x10^{-3}$	0.9719	9.23	5.6
Sample 4	-----	-----	-----	0.9435	0.0531	$2.6x10^{-2}$	0.8242	5.34	2.6
Sample 5	0.9055	0.0088	$3.3x10^{-3}$	0.8827	0.0093	$3.9x10^{-3}$	0.8454	5.79	2.6
Sample 6	-----	-----	-----	0.7688	0.1609	$2.4x10^{-2}$	0.8387	7.50	3.3